

Pyrite Geochemistry and Textures in the Epithermal Au-Ag Mineralisation at Waihi

A G Eames¹, S LL Barker¹ and P M J Durance²

¹University of Waikato, School of Science, Private Bag 3105, Hamilton. Email: anna_eames@hotmail.com

¹University of Waikato, School of Science, Private Bag 3105, Hamilton. Email: sbarker@waikato.ac.nz

²GNS Science, PO Box 30368, Lower Hutt. Email: p.durance@gns.cri.nz

Abstract

The Waihi epithermal system is a low sulphidation epithermal system that hosts one of the largest high grade ore deposits in the Southern Hemisphere. The use of petrographic and EPMA analyses demonstrate there are distinctive textural zones within pyrite grains that vary in chemistry and appearance. Some of these zones contain elevated concentrations of Au and Te, and varying concentrations of Fe, S, Cu, Pb or Zn. The textural observations indicate that in some samples, pyrite growth was interrupted by periods of dissolution. Grains begin growth with overall low trace element concentrations, with the highest concentrations of trace elements occurring in the middle phase of the grain's growth. Inclusions are rich in Pb, Ca, Se, Zn and Ni, and are attributed to the 'dirty' texture of some samples. Inclusion-rich areas are also high in Au. The nature of the presence of Te suggests either a single source of magmatic fluid, released in pulses, or periodical dilution of the magmatic fluid by meteoric waters.

Keywords: Waihi, epithermal, pyrite, invisible gold, trace elements, magmatic, sulphidation, chemistry, texture.

Introduction

Gold and silver are found within electrum, but gold can also occur within pyrite and is referred to as "invisible" gold (Myagkaya et al., 2016). This paper focuses on the textures and chemistry of pyrite (FeS₂) due to its abundance and ability to incorporate various trace metals within its structure (Large et al., 2009). Pyrite forms in epithermal settings by the passing of sulphide-bearing hydrothermal fluid through iron-bearing host rocks producing a sulphidation reaction that results in the growth of pyrite. The crystal structure of pyrite allows trace elements present in the hydrothermal fluid to be incorporated in the pyrite grain chemistry (Deol et al., 2012). As the fluid chemistry changes, so too does the pyrite inclusion chemistry growing from the fluid. This creates a zoned appearance under reflected light microscopy. In low sulphidation systems, zoning in pyrite is less common, and pyrite grains are commonly relatively homogenous (Arribas Jr, 1995). The precious metal inclusions in the pyrite crystal structure are often not visible to the naked eye or under reflected light microscopy and detection of these metals is accomplished via SEM or LA-ICPMS analysis (Deol et al., 2012).

This paper examines the occurrence of zoning in pyrite grains from drill holes from the Martha Vein, Waihi. The chemistry of each zone in the pyrite grains is analysed and compared, with special interest focused on the concentration of Au and Ag and the presence

of Te. Tellurium is of interest because it can be a reliable indication that there has been an influence of magmatic fluid in the epithermal system (Simmons et al., 2016). Elevated concentrations of Te at Waihi would support the theory that Waihi was an epithermal system subjected to magmatic fluid at times in its history (Arribas Jr, 1995; Brathwaite & Faure, 2002). The presence of Au and Ag is of economic interest, as well as being used as indicators for gold forming stages. The placement of the Au and Ag, relative to the changing trace element chemistry of the pyrite zones can be used as an indicator for the fluid composition at the times of gold formation (Deol et al., 2012). Analysis is undertaken using bleach etching to first identify pyrite zonation. Electro-Probe Micro Analysis (EPMA) was then carried out to determine the composition of the observed zoning patterns. These analyses enabled us to identify recurring zoning patterns and geochemical trends.

Waihi Epithermal System Mineralogy

Epithermal Setting

The Waihi epithermal system is a gold-silver-base metal sulphide-quartz vein system (Brathwaite & Faure, 2002). The system is hosted in andesites and dacites of the Coromandel Group. The geology of the area is illustrated in Figure 1 with the areas of concentrated mining interest shown to be in the altered andesite. The main ore minerals of the system include electrum and acanthites (commonly associated with pyrite, sphalerite, galena and chalcocopyrite).

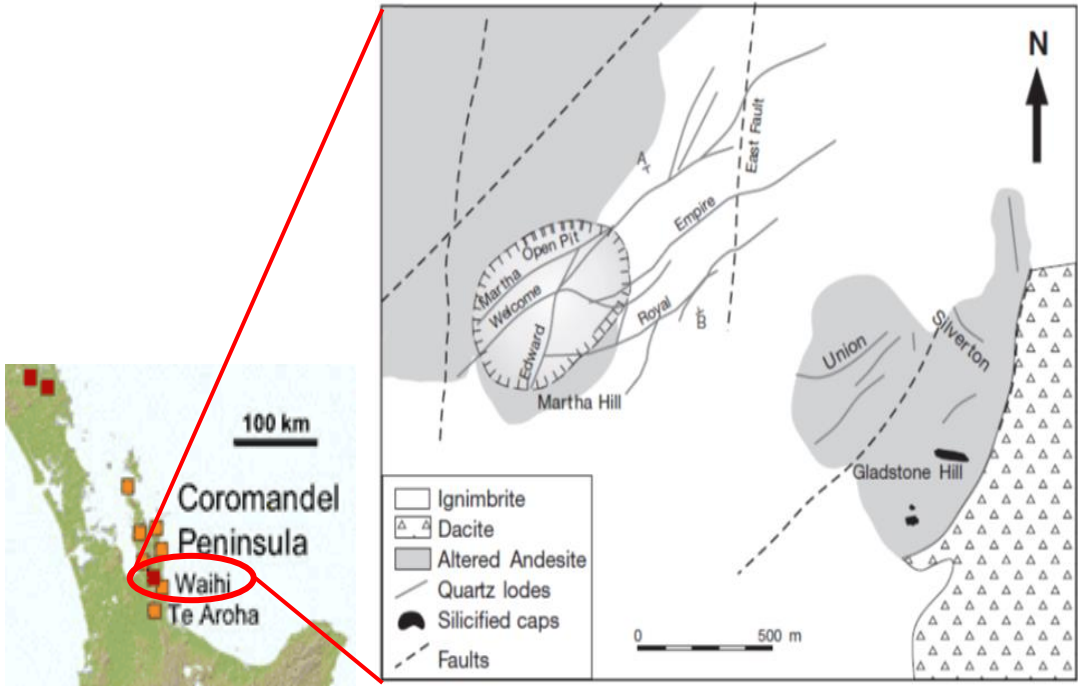


Figure 1: Geologic map of Waihi. Lodes below ground are projected to the surface. Modified from (Brathwaite & Faure, 2002).

Alteration Mineral Assemblages

Previous studies on fluid inclusion data from similar deposits in the Coromandel Volcanic Zone suggest that the base metal sulphides were deposited from fluids at high temperatures (260°-320°C) and a salinity of 1.7-6 wt% NaCl equivalent, comparatively higher than the electrum bearing sulphide ore (Brathwaite & Faure, 2002). The Waihi alteration structure indicates how the hydrothermal activity affected the local area. Three alteration zones are apparent in the Waihi system: (1) a smectite zone composed of smectite-chlorite-calcite-pyrite, (2) an interlayered illite-smectite zone, and (3) an illite zone with adularia-quartz-illite subzone, adjacent to the quartz lodes. In the least altered zone (1), magnetite is altered to pyrite + titanite. With increasing intensity of alteration, the plagioclase is altered to chlorite + calcite + pyrite, which occurs mostly in the upper part of the vein system on the hanging wall of the Martha lode, especially to the eastern end of the deposit. In the zone of strongest alteration, the groundmass of the rock consists of mosaic quartz, illite, minor interlayered illite-smectite and disseminated pyrite (Brathwaite & Faure, 2002).

Mineralisation

The vein mineralisation at Waihi consists of multiple vein phases filled with quartz (microcrystalline to medium grained), and quartz vein breccias. Pyrite, sphalerite, galena, chalcocite, and acanthite occur mostly in the form of sulphide bearing bands in fine to medium grained quartz. Microcrystalline colloform quartz comprises most of the shallow vein fill, occurring as colloform and crustiform bands. The colloform quartz contains minor pyrite, sphalerite, chalcocite, tetrahedrite, acanthite, and electrum. At depth, the colloform quartz grades to crustiform comb quartz and sulphides (Brathwaite, 2005).

The fluids present during the hydrothermal activity at Waihi are thought to be a mixture of deep chloride-rich fluid and steam-heated meteoric water (Brathwaite & Faure, 2002). The deep water compositions suggest that redox conditions within the system are constrained by the equilibrium between pyrite and Fe chlorite. Some of the reduced waters corresponds to pyrite-pyrrhotite equilibrium and is attributed to local incorporations of steam and relatively high H₂/H₂S ratios (Simmons & Browne, 2000).

The Waihi epithermal system has been shown to have several stages of evolution. The first stage was an initial vein filling with platy calcite, quartz, pyrite and adularia. This is associated with the alteration of the andesite wall rock. The wall rock alteration associated with the first stage is characterised by a proximal mineral assemblage of adularia + quartz + pyrite (Brathwaite & Faure, 2002). The second stage is a main stage of vein filling by quartz and sulphides, with or without electrum. The final stage is of vein deposition is minor amethyst.

Analytical Techniques

Analysis of the pyrite grains was carried out on polished and mounted, epoxy rounds. The pyrite grains were identified using reflected light microscopy and were marked on photographs. Pyrite grains were etched with 5% sodium hypochlorite for 45 seconds and then rinsed with water to highlight their internal zoning under reflected light microscopy.

Nine individual round 1 inch epoxy mounts were analysed. The pyrite grains with identified zoning were analysed on the JEOL JXA-8230 SuperProbe Electron Probe Microanalyser at Victoria University of Wellington. The analyses were done using a 1 μ m spot on the different zones for 8 minutes per spot. The measurements were compared to an Elba pyrite standard and pure metals for the various elements to define peak and background positions, and assess appropriate counting times to achieve as low a detection limit as practicable. The Virtual WDS software (Cambridge) was used for determining best crystals and peak positions to avoid elemental overlaps. The specific elements selected for were Bi, Au, W, Mo, Fe, As, Si, Zn, Co, Cu, Se, Pb, Sn, V, Ca, Sb, Te, Ni, Hg, Ag and S. The data was obtained at 20 KV and 10 nA for major elements, 100 nA for trace elements, with detection limit set at 59 to 70 ppm. The data was then examined using ioGAS software to identify any trends and element relationships.

Results

Zoning Textures

Under reflected light microscopy, and with application of the bleach etching method, the pyrite grains were shown to vary texturally within individual grains and no clear pattern is evident between samples.







The grains within samples are grouped based on their texture classification. The groups are named in such order; (zoning occurrence), (zoning type), (zoning shape), and are discussed in greater detail in Table 1.

Trace Element Analysis

Figure 2 shows there is a positive relationship between elevated As and elevated Au concentrations in the pyrite. However, in the most extreme case of high Au concentration the As concentration is below detection. The relationship between As and Au can be described as very weak, based on the distribution of points, with outliers favouring a higher Au concentration. There is a cluster of points that show variable amounts of Au (0.006-0.02%), with an As concentration below detection.

The concentration of Au varies across the sample's different zones. Figure 3 shows that the Au concentration across the grain is initially at the lowest concentration of 0.006% before spiking up to the highest 0.022% and then gradually decreasing.

Table 1: Results of the bleach etching showing the different types of zoning.

Zoning Type	Main Characteristics	Example
Clean, Radial (CR)	Grains in this group display a tree ring like zoning pattern. Each zonation is sharply defined, straight (no jagged or wavy edges) and parallel with the crystal faces of the grain. Grains of this group are generally the larger grains in the sample, and are around 300µm.	
Dirty, Radial (DR)	These grains are similar in appearance to the CR group grains however, the zonations are wider (i.e. there are fewer zones) and the edges of each zonation are more diffuse, making them more difficult to define. Within each band there may also be some pitted textures that give the grain a dirty appearance.	
Clean, Planar (CP)	The grains in this group have clearly defined zones of differing colour that are not the same shape as the grain itself suggesting new pyrite growth around a pre-existing pyrite grain. Often these zone textures apply to one side of a grain or have an apparently random occurrence. These grains are similar in size to DR and CR. Does not follow grain shape.	
Dirty, Planar (DP)	This group is similar in appearance to the CP grains. The edges of each colour zone are not clear or easy to define. Within each zone there may also be some large pitted textures. The darker coloured zones are commonly dirtier than the lighter zones. Zones do not follow grain shape.	
Clean, Bordered (CB)	These grains have the same characteristics as the CR grains. The zoning in this group is limited to two distinct zones, creating a border appearance. The border follows the inner shape of the grain, with the outer grain edge is sometimes parallel, but often displays poor formation of crystal faces.	
Dirty, Bordered (DB)	These grains have a similar appearance to the CB grains. However, they are not as obvious under reflected light, as the colour change can be very slight. Also, the dirty, pitted textures of the grain can obscure the recognition of the zonations. Within each zone there may also be some dissolution and the grain surface can look pitted. The darker coloured zones are commonly dirtier than the lighter zones.	

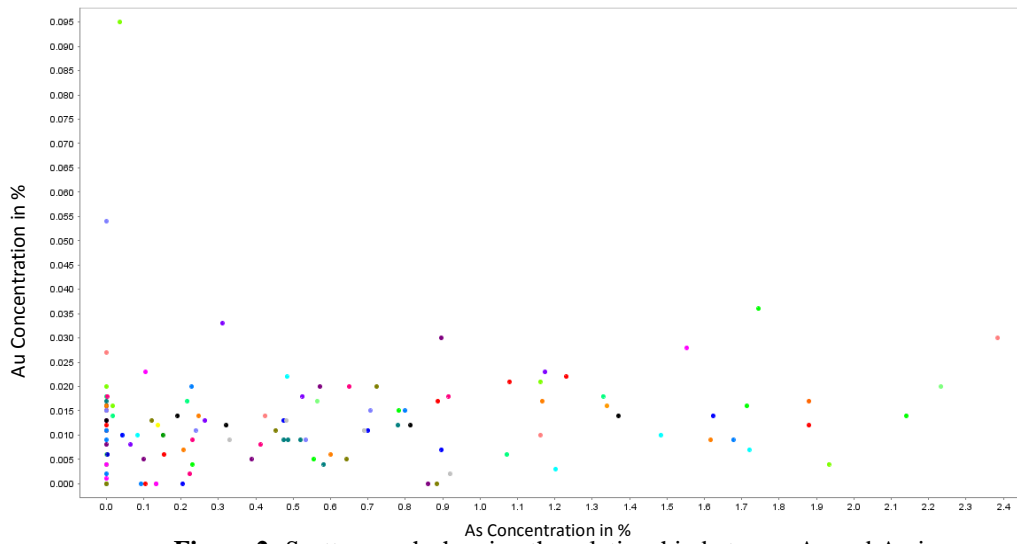


Figure 2: Scatter graph showing the relationship between As and Au in ppm. The colours of the different dots are associated with their specific sample.

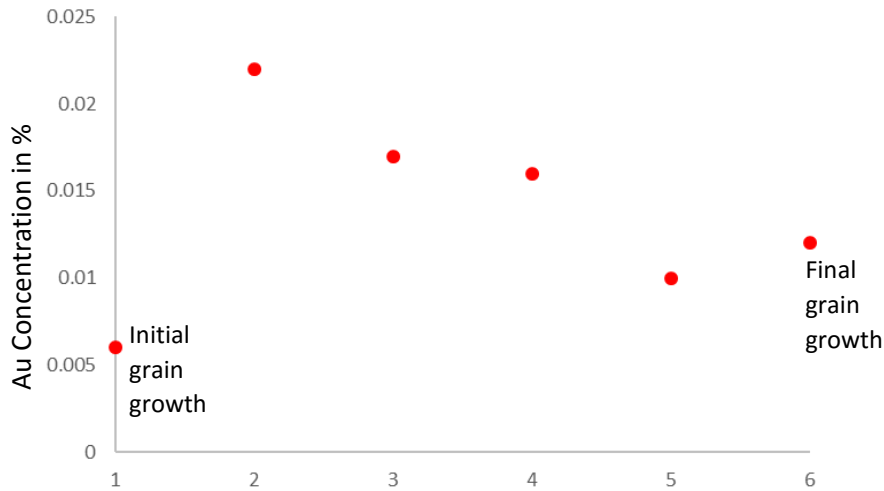


Figure 3: Graph depicting the varying concentrations across the different zones of sample AU57390B_Z1. The points are labelled 1-6, with 1 being the most central part of the grain, and 6 the outer edge. The detection limit for Au is 0.011%.

Figure 4 below shows there is a presence of Te in the grains at Waihi. Most of the samples have little to no Te, but few show higher concentrations up to 0.012%. There does not appear to be any trend; the occurrence of Te is not clustered within single samples.

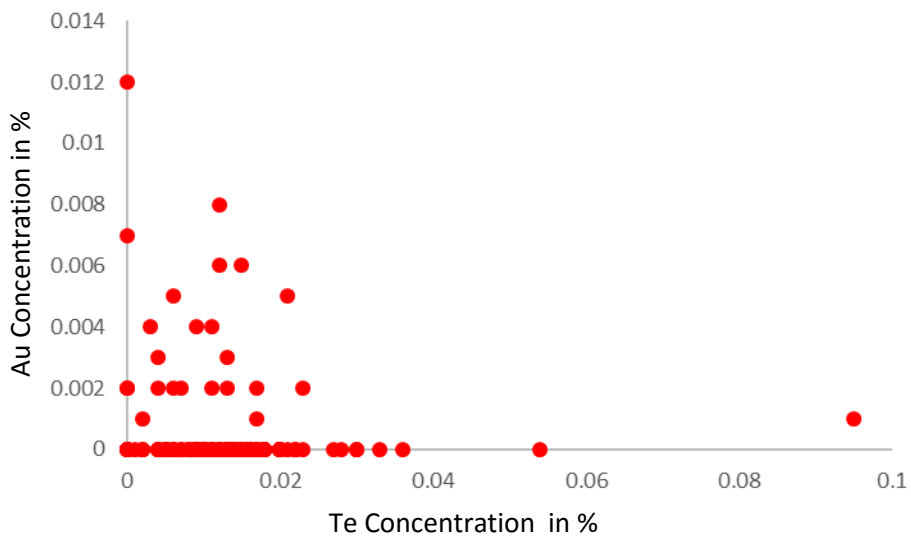


Figure 4: Graph of Te vs Au concentrations across all tested samples. Te detection limit is 0.005%.

Discussion

Heterogeneity of Zone Geometry

In the results section above, texture has been used to identify six different types of zoning. The first type mentioned is CR, where the interior of the grain resembles a tree ring like structure. This suggests that the grain experienced continual growth with no dissolution from the time of initial crystallisation. The ring like structure implies a variable chemistry, over time, in the passing fluids (Zhu et al., 2011). In the case of the DR zoning, the conditions of growth are the same. The dirtiness is a result of inclusions within zones, creating a pockmark appearance under reflected light microscopy. EPMA results of DR are very different compared to CR. This is a result of very different chemistry within the dirty zones, owing to the presence of inclusions (Thomas et al., 2011).

CP and DP zoning are both unexpected, as they do not follow the theoretical outcome of grain growth from passing fluids. Grains are expected to show a radial pattern, due to the fact that they are growing from a central nucleus, outwards. This should result in the tree ring structure common in Carlin-style deposits (Large et al., 2009). However, for some reason, zones in grains have been found that do not reflect the geometry of the grain itself on a visual scale. This could be for a number of reasons; the grain may have been cut at an angle that does not show the zoning to be radial. There could also be some alteration to grains such as dissolution, over-growths, grain clusters or precipitation after they have formed, causing the patchiness seen, especially evident in sample AU57417, the DP example, Table 1.

CB and DB are similar in growth history. These textures suggest two stages of growth associated with a different fluid composition. These grains only show two zones texturally, with the apparent change in fluid chemistry not coming until close to the edge of the grain. The dirtiness again comes from inclusions (Thomas et al., 2011).

Inclusion Chemistry

The samples DR, DP and DB all exhibit the same dirtiness. This is potentially from the result of the grain growing, then partially dissolving, then growth recommencing. The dirtiness indicates possible inclusions of partially dissolved pyrite mixed with elements from the fluid that the pyrite dissolved in. This is supported by the Figure 5 below.

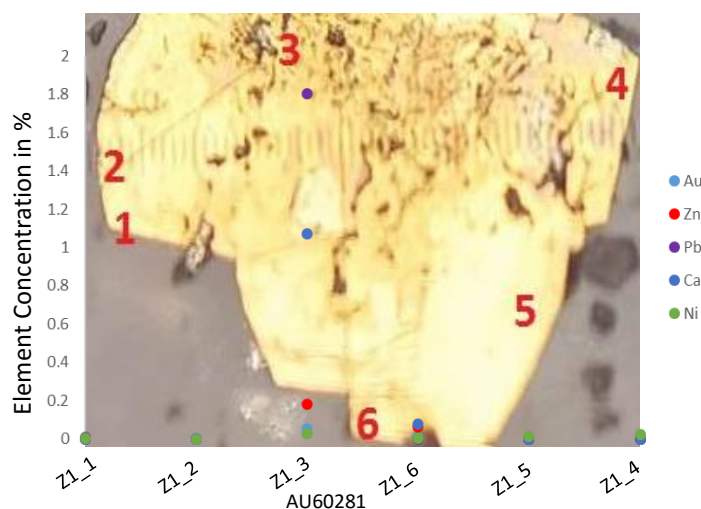


Figure 5: Graph depicting the concentration spike where inclusions were suggested. The points refer to the analysis points on the grain. The colours are; purple=Pb, blue=Ca, red=Zn, light blue=Au, green=Ni.

The sudden spike in element concentration at point 3 corresponds to the dirty looking centre of the grain. The samples in figures CR, CP and CB show no evidence of having undergone any dissolution, and this is reflected in the data in Figure 3 where the Au concentration drops at a steady rate.

Grain Growth

The chemical variances in the grains are reflected in the colour and textural differences, as shown by Figure 6 below; the rise in Au concentration is accompanied by a darker colour zone. In Figure 5 above, the texture gets dirtier with the presence of a larger variety of elements. The history of the growth of the grain in Figure 6 is suggested to be initially low in trace elements, with an influx of gold-rich fluid at point 2. After the gold-rich influx, the fluid gradually decreased in gold for the rest of the grain's growth. This one sample suggests that gold deposition occurred as a single event. This is expected to be accompanied by a drop in sulphide in solution, which may be visible in the data, however, further work must be done (Large et al., 2009). Whether this particular fluid chemistry was experienced by other samples in the Martha system will require more study.

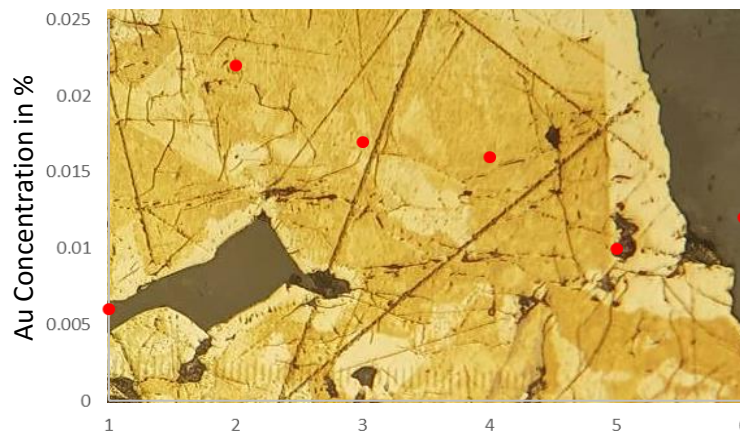


Figure 6: Graph depicting the varying concentrations across the different textural zones of sample AU57390B_Z1. The points are labelled 1-6, with 1 being the most central part of the grain, and 6 the outer edge.

Fluid Chemistry

The chemistry of the fluid at periods of high gold deposition can be assumed to be high in As also, suggested by the positive relationship shown in Figure 2. This is different to the typical arsenian pyrite-Au relationship seen in other deposit types such as Carlin style (Large et al., 2009). There does not at this stage in the research appear to be a relationship between any other trace element analysed and the Au concentration.

Further Work

Further work will be done on connecting the samples and their gold-rich phases in space. Creating a spatial model of the samples, linking those with zones of high Au concentration, will provide insight into the fluid processes and chemical history of the Waihi epithermal system. We will need to determine whether chemical phases in single grains can be connected with chemical phases in other grains. One aim is to note how many individual high gold zones there are within grains, and if any of the grains sampled have more than one

distinctive high gold zone. We also plan to identify the changes in the fluid chemistry before and after gold deposition, noting especially any variations in Te.

Conclusions

The main visible variations between zones in the pyrite grains at Waihi appear to be attributable to variable trace element concentrations. Elevated Au is associated with zones of a darker colour, while dirty textures are attributed to inclusions rich in Pb, Ca, Se, Zn and Ni. The variety of textural differences between samples is suggestive of multiple chemical changes spatially and during grain growth throughout the system. The presence of Te suggests the influence of magmatic fluid in some of the grains providing evidence for the long suspected theory that the Waihi epithermal system was influenced by magmatic fluid.

Acknowledgements

This study was made possible thanks to the generous funding from the Ministry for Business, Innovation and Employment, UoW, GNS, AusIMM, SJ Hastie Award and the Broad Memorial Fund. A special thank you to Dr Ian Schipper for all the help in the laboratory with the EPMA and Steve Cameron for his help with the LA-ICPMS.

References

- Arribas Jr, A. (1995). Characteristics of high-sulphidation epithermal deposits, and their relation to magmatic fluid. *Mineralogical Association of Canada Short Course*, 23: 419-454.
- Braithwaite, R.L. and Faure, K. 2002. The Waihi epithermal gold-silver-base metal sulphide-quartz vein system, New Zealand: temperature and salinity controls on electrum and sulphide deposition. *Economic Geology*, 97(2): 269-290.
- Braithwaite, R. 2005. The Martha Hill epithermal Au-Ag deposit, Waihi—geology and mining history. *Geology and Exploration of New Zealand Mineral Deposits*, AusIMM Monograph, 25:171-178.
- Deol, S., Deb, M., Large, R.R. and Gilbert, S. 2012. LA-ICPMS and EPMA studies of pyrite, arsenopyrite and loellingite from the Bhukia-Jagpura gold prospect, southern Rajasthan, India: implications for ore genesis and gold remobilisation. *Chemical Geology* 326: 72-87.
- Large, R.R., Danyushevsky, L., Hollit, C., Maslennikov, V., Meffre, S., Gilbert, S. and Thomas, H. 2009. Gold and trace element zonation in pyrite using a laser imaging technique: implications for the timing of gold in orogenic and Carlin-style sediment-hosted deposits. *Economic Geology* 104(5): 635-668.
- Myagkaya, I.N., Lazareva, E.V., Gustaytis, M.A. and Zhmodik, S.M. 2016. Gold and silver in a system of sulphide tailings. Part 1: Migration in water flow. *Journal of Geochemical Exploration* 160: 16-30. doi: <http://dx.doi.org/10.1016/j.gexplo.2015.10.004>
- Simmons, S.F., Brown, K.L. and Tutolo, B.M. (2016). Hydrothermal transport of Ag, Au, Cu, Pb, Te, Zn, and other metals and metalloids in New Zealand geothermal systems: spatial patterns, fluid-mineral equilibria, and implications for epithermal mineralisation. *Economic Geology*, 111(3): 589-618.
- Simmons, S.F. and Browne, P.R.L. 2000. Hydrothermal minerals and precious metals in the Broadlands-Ohaaki geothermal system: Implications for understanding low-sulphidation epithermal environments. *Economic Geology and the Bulletin of the Society of Economic Geologists*, 95(5): 971-999. doi: 10.2113/95.5.971
- Simmons, S.F., White, N.C. and John, D.A. 2005. Geological characteristics of epithermal precious and base metal deposits. *Economic Geology 100th anniversary volume*, 29: 485-522.
- Thomas, H.V., Large, R.R., Bull, S.W., Maslennikov, V., Berry, R.F., Fraser, R. and Moye, R. 2011. Pyrite and pyrrhotite textures and composition in sediments, laminated quartz veins, and reefs at Bendigo gold mine, Australia: insights for ore genesis. *Economic Geology*, 106(1): 1-31.
- Zhu, Y., An, F. and Tan, J. 2011. Geochemistry of hydrothermal gold deposits: a review. *Geoscience Frontiers*, 2(3): 367-374.